

RPN 23

2

LABORATORY OF PLASMA STUDIES  
CORNELL UNIVERSITY  
ITHACA, NEW YORK

AN INITIAL STUDY ON THE PROPAGATION OF A  
HIGH CURRENT RELATIVISTIC ELECTRON BEAM

by

M. L. Andrews, J. J. Bzura, H. E. Davitian, H. H.  
Fleischmann and D. A. Hammer, Laboratory of Plasma  
Studies, Cornell University.

I. M. Vitkovitsky and L. S. Levine, Naval Research  
Laboratory.

LPS 15

SEPTEMBER 1969

This work was supported by the U.S. Office of Naval Research under  
Contract No. N00014-67-A-0077-0003.

## ABSTRACT

The transport of relativistic electron beams consisting of up to 500 keV electrons in tens of kiloampere currents has been examined in an introductory experiment with background air pressures of 0.1 to 2.0 torr. These beams were guided in 14cm-diameter metal-mesh-lined lucite drift tubes, typically 6.4 meters long. Their properties were determined through (a) time-resolved measurements of diode voltage and current, (b) x-rays from primary electrons hitting targets along the drift tube walls and at its end, (c) prompt visible light radiated from the beam system recorded in streak photography, and (d) magnetic fields of the total current within the drift tube. Beam-transit times given by these measurements proved to be considerably longer than the straight-line transit of 300 keV electrons, especially at lower pressures. The total current within the drift tube was found to be less than the injected primary electron current, indicating that a large return current was flowing in the beam-produced background plasma that partly canceled the beam current. In the streak photography a striation-like structure was recorded in the light output from the beam and the node-node distance separating these striations varied inversely as the pressure. The implications of these results on possible models for beam propagation are discussed.

## Introduction

The recent development of systems capable of producing intense relativistic electron beams of hundreds of kilo-electron volts and tens of kiloamperes has stimulated anew an interest in understanding the propagation of these beams. Early models for these beams were derived by Bennett, [1] Alfven [2] and Lawson.[3] In the case first worked out by Alfven and later expanded by Lawson, the form of electron orbits is calculated for assumed self-fields of the beam. If one allowed some neutralization fraction of background ions within the beam, then it was possible to find solutions where the reduced electrostatic repulsive force was balanced by the cohesive force of the self-magnetic field and the beam would be transported. However, if the beam current was increased, the electrons would form trajectories with increasing transverse components. Ultimately, even with complete neutralization, a critical current,  $I_c = 17,000 \beta \gamma$  amps, would be reached where the electrons have lost all net forward motion. This condition implied that electron beams might not be able to propagate for currents above  $I_c$ ,  $\beta$  is the ratio of electron speed to the speed of light and  $\gamma = (1 - \beta^2)^{-\frac{1}{2}}$ . First experiments seemed to be contradictory in this regard, showing a catastrophically stopped beam [4] in one case and a smoothly propagating beam in experiments at Cornell. [5]

These early experiments had little or no time-resolved diagnostics along the drift tube. Data were obtained predominately by integrated measurements from calorimetry, blue cellophane dosimetry, x-ray dose from end targets, open-shutter photography and target damage. [6,7,8,9,10,11,12] It was discovered that with appropriate beam parameters and background pressure the energy transported by the beam indicated fast-electron currents in excess of  $I_c$ . These results stimulated further theoretical investigation of high-current beams. A steady-state representation for these beams without external fields was developed by Hammer and

Rostoker [13]. This relativistic self-consistent field solution resulted in a shell-current distribution allowing currents in excess of  $I_c$ . However, experimental evidence indicated that the current flowing within the drift tube was considerably smaller than the primary electron current. [6,12] This problem was also examined by Hammer and Rostoker, [13] who considered the acceleration of secondary electrons produced at the front of the beam and showed that a current is set up with the secondary electrons opposite to the primary current that is capable of canceling a large fraction of the magnetic field within the beam. This lower effective magnetic field leads to the possibility again of transporting more intense beams.

The experimental investigation concurrent with this theoretical study required a much more detailed examination of the beam, both in time and in position along the beam, than the early time-integrated measurements had accomplished. This investigation required longer drift tubes than the typical one-meter tubes previously employed and the addition of a number of diagnostic stations along the drift tube. More importantly, it necessitated time-resolved measurements in order to obtain transport parameters such as the propagation velocities. The data presented in this paper represent the first results of experimentation directed toward the development and utilization of time-resolved diagnostics on intense relativistic electron beams. Our studies employed simultaneous use of the following techniques: (a) scintillator diodes to detect x-rays from beam electrons impinging on metal foils, (b) calorimetry to measure the total energy incident on the end of the drift tube, (c) streak photography to record the fast-light emission during and in the wake of the electron beam and (d) small loop probes to yield the magnetic fields just inside the drift-tube liner. This procedure resulted in a number of

independent determinations of beam-transit time showing periods that were always greater than those for straight trajectories and that increased in duration at lower pressures. An unexpected nodal phenomena, relatively stationary in the laboratory frame, was indicated in the streak photography, with a repetition distance inversely proportional to pressure. The results from these experiments were reported in part at the American Physical Society Plasma Division Meetings at Miami [14,15] and more completely at the recent Conference on Intense Relativistic Electron Beams, sponsored by the Naval Research Laboratory and held at Cornell University.

#### Electron Beam Measurements

##### Experimental Arrangement:

The basic set-up utilized in this investigation is shown in Figure 1. A surge generator charges the mylar pulse-forming line and after a solid-dielectric switch of polyethylene closes, a four-ohm source, 50-nsec pulse is applied to the diode. [16] The electrons streaming from the cathode penetrate the anode foil to form the electron beam propagating in the drift tube. This beam has a rather uniform distribution, typically about 10 cm in diameter, reflecting the size of the planar cathode usually employed. [17] The entrance-angle distribution of the beam is believed to be dominated by scattering in the anode foil with about a twenty-degree half angle.

The drift tube has a 14 cm inner diameter and is lined with number 18 mesh aluminum screen. In this case a 6.4 meter length of tube was used and filled with air to a desired background pressure. Three scintillator diodes were employed. Two detected x-rays from tantalum foil strips placed on the wall between the screen and the lucite. One strip was 0.6 m and the other 3.0 m down the tube

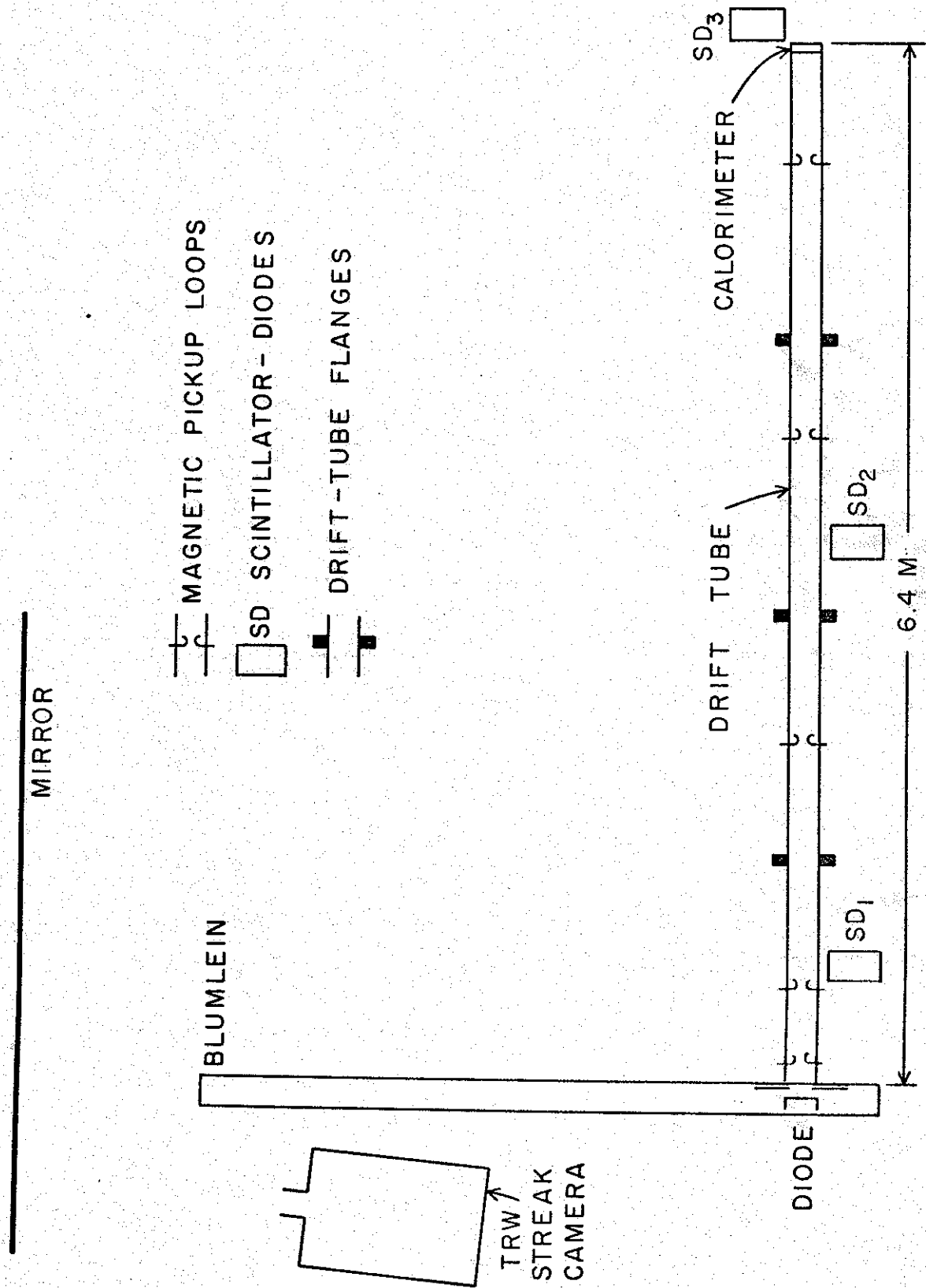
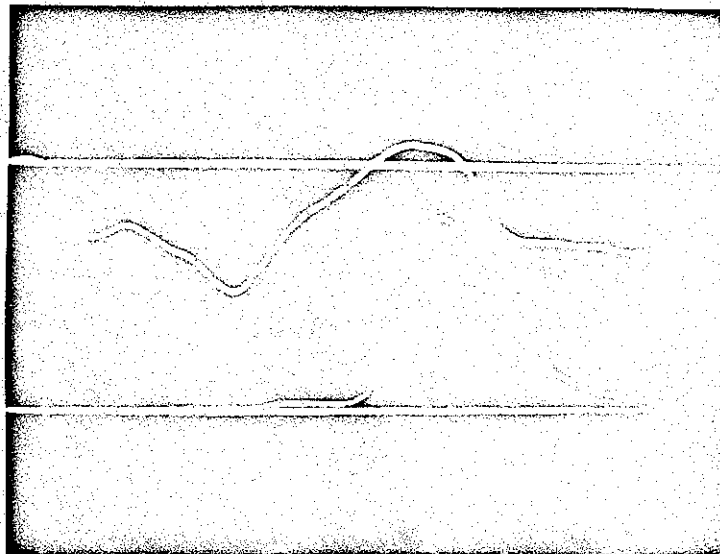


Figure 1 Experimental arrangement for initial investigation of intense relativistic electron beams with time resolved measurements.

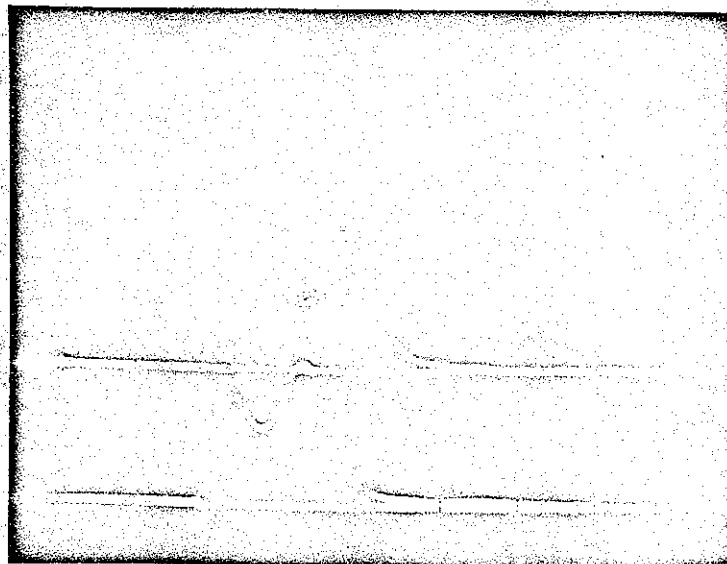
away from the anode foil. The third scintillator diode was positioned so that it sensed the x-rays from the aluminum calorimeter plate covering the end of the drift tube. A streak camera viewed the entire drift tube through a mirror to give a long-path length and the image of this drift tube was swept across the photograph with time. Five doublet magnetic field probes are deployed along the drift tube at distances 0.1, 0.7, 1.9, 4.1 and 5.0 m from the anode foil. Data were taken concurrently with all of these diagnostics in a series of shots where the pressure was varied from 2.5 torr to 0.10 torr. The diode voltage was typically 350 kV, the diode current about 30-50 kA and a 1-mil titanium anode foil was used throughout the series.

#### X-ray Scintillator Diodes and Calorimetry.

Each scintillator diode consists of a 10-cm diameter, 8-cm long, polished piece of Pilot B plastic scintillator tapered at one end to allow an optical grease fit to an I.T.T. Industrial Laboratories type FW 114 fast photodiode. This scintillator diode is then placed in a cylindrical metal container, packed with magnesium oxide. The cylindrical container, which serves as an inner shield, is then enclosed with another metal box to form a second shield. Batteries are used to power the photodiode tube. This system has about a 4 nsec response time and a linear output up to 100 volts. Typical oscilloscope traces for the outputs of these scintillator diodes are shown in Figure 2. In the first picture the top trace represents the diode current measured with a series resistance between the anode foil and the grounded anode side of the pulse line, [17] while the lower trace is the output from the scintillator diode at the end of the drift tube detecting the x-rays from the aluminum calorimeter plate. Trace pairs are synchronous



The upper trace is from the current monitor with 27 kA/div and the lower trace is from the scintillator diode at the end of the drift tube. The sweep is 20 nsec/div.



These traces are from the wall foil scintillator diodes; the upper is 0.6 m and lower is 3.0 m from the beginning of the drift tube. The sweep speed is 40 nsec/div.

Figure 2 Scope signals from the current monitor and scintillator diodes. In this case there was 1.35 torr of air in the drift tube and the initial electron energy was 320 keV.



in time and swept at 20 nsec/div with a 7-nsec risetime dual-beam oscilloscope. In the second picture the traces record the output of the two scintillator diodes detecting the x-rays from the 3 mil tantalum foils at the walls. The upper trace, for the foil 0.6 m from the diode, is time-synchronized with the lower trace, for the foil 3.0 m from the diode, both traces having an oscilloscope-limited rise time of 11 nsec. A 2.5-nsec rise time oscilloscope was also used for the upper trace and showed rise times as low as 6 nsec, so that these traces were oscilloscope-limited on the initial rise.

Figure 3 shows the transit-time data obtained from scintillator diode traces in this series, normalized to a 6.4 meter distance. The solid line shows the transit time represented by the delay between the half heights of the first peaks for the traces from the wall foils. Transit times for the bulk of the beam electrons are given by the upper and lower dashed lines which are derived from the delay between the half heights of the rise and fall respectively of both the diode current and the x-ray signal at the end of the drift tube. There is a marked difference between the transit times normalized to the full-tube length from the wall foils and that marked by the x-rays at the end of the drift tube. It is found that for higher pressures, around 2 torr, there is a small early-step signal, before the bulk of the electrons arrive, which is just visible in Figure 2, and for low pressure, around 0.15 torr, there is a small residual step-down signal after the primary signal. If these are used as the beginning and end of the x-ray signal, instead of the half rise and fall times, then the discrepancy is substantially alleviated. One notable feature of the end-scintillator diode traces is that the half width of the bulk of the electrons is approximately a constant of twenty nanoseconds, independent of pressure. Also, the double-peaked traces of the wall-foil x-rays

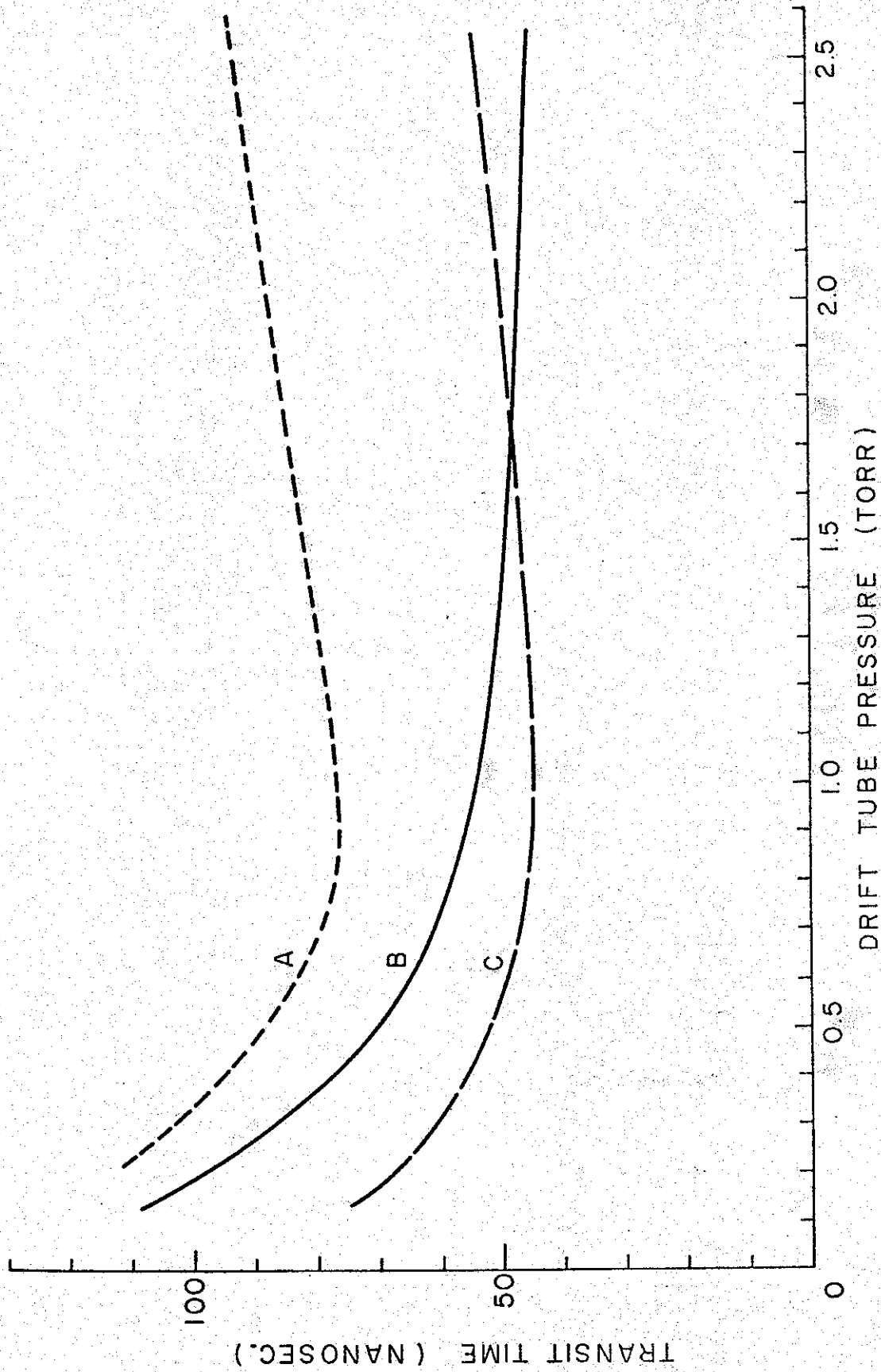


Figure 3 Beam transit time versus pressure measured by the scintillator diodes detecting x-rays from wall foils and the end target. These transit times have been linearly normalized to a 6.4 m drift tube length. The line designated (b) is the transit time measured from the wall foils; (a) the half rise of the diode current compared to the signal half rise from the end target; and (c) the half fall points for these two signals.

are typical of their behavior and the peak separation is approximately independent of pressure. However, there appears to be no obvious relation between the ratios of peak heights.

The amplitude of the end-scintillator diode is a strong function of pressure as indicated in Table 1. The calorimeter at the end of the drift tube was a single-element device, consisting of a 0.79 mm thick aluminum plate with a diameter nearly equal to that of the drift tube and a chromel-alumel thermocouple imbedded in its center. In Table 1 the dependence of the calorimeter measurements on pressure is shown where both the calorimeter and scintillator are normalized to the diode input. These normalizations were obtained first by calibrating the calorimeter and scintillator diode directly in front of the anode foil, dividing the calorimeter data by the diode beam energy  $\sqrt{V_0 I_0 \tau}$  and the scintillator diode data by the empirically determined dose dependence  $V_0^2 I_0$ . [11] Then with the calibrations of the outputs, the results at the end of the drift tube could be compared by normalizing again with the diode measurements. A ratio of the normalized scintillator diode and calorimeter outputs, multiplied by the ratio of the duration at the end of the drift tube to the diode-pulse duration at the start, gives an estimate of the electron energy at the end of the drift tube compared to the initial energy. This is calculated in the last column of Table 1 and indicates, albeit rather coarsely, that the electron energy at the end of the drift tube is about one-third of the input.

#### Streak Photography

A TRW Image-Converter Camera with the Wide-Range Streak plug-in was used for streak photography of the beam. Through mirrors the effective path length was increased to 26 meters, so that the long narrow drift tube simulated a slit and


TABLE I  
 RELATIVE ENERGY REACHING THE END OF THE 6.4 M DRIFT TUBE

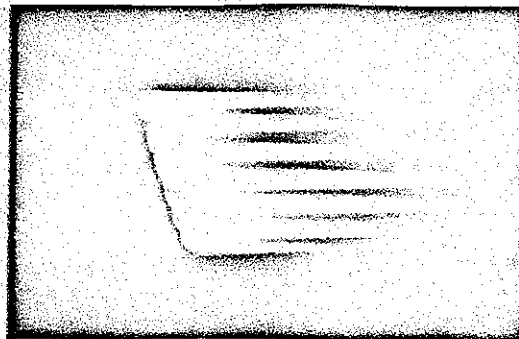
| PRESSURE   | CALORIMETER<br>$\frac{S-D}{VI \tau_1}$ | SCINTILLATOR-DIODE<br>$\frac{S-D}{VI \tau_1}$ | $\left( \frac{S-D}{VI \tau_1} / \frac{CALOR}{VI \tau_1} \right) \tau_1$ |
|------------|----------------------------------------|-----------------------------------------------|-------------------------------------------------------------------------|
| 2530 $\mu$ | 0.21                                   | 0.18                                          | 0.28                                                                    |
| 1850       | 0.23                                   | 0.28                                          | 0.40                                                                    |
| 1400       | 0.25                                   | 0.36                                          | 0.47                                                                    |
| 880        | 0.23                                   | 0.24                                          | 0.35                                                                    |
| 600        | 0.22                                   | 0.23                                          | 0.35                                                                    |
| 400        | 0.18                                   | 0.20                                          | 0.36                                                                    |
| 310        | 0.11                                   | 0.12                                          | 0.35                                                                    |
| 255        | 0.10                                   | 0.10                                          | 0.34                                                                    |
| 135        | 0.02                                   | 0.02                                          | 0.3                                                                     |

the image of this drift tube on the film, about 22 mm x 0.5 mm, was streaked perpendicular to its length across 5 cm of film in 500 nsec. The camera and power supply were shielded from x-rays with over a centimeter of lead and both were operated inside conducting boxes to double-shield them and cut down on electromagnetic pick-up. A trigger was produced for the streak by means of a 30-cm diameter loop of styroflex cable with the center wire at the cable end connecting back to the cable shield to form the loop. This detector was suspended above the pulse line near the switch area to obtain a magnetic-field-induced voltage pulse which, because of the optical delay, had ample time to start the sweep and photograph the very beginning of the beam's transit down the drift tube. [18]

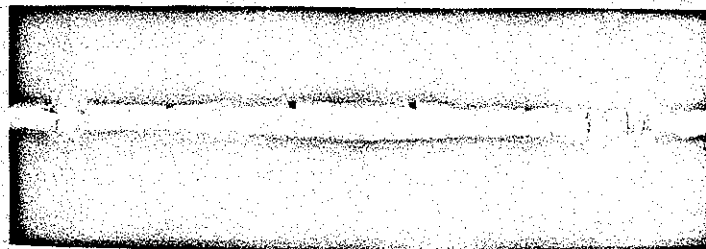
A typical streak photograph is shown in Figure 4. The image of the drift tube would resemble a small vertical bar that is swept to the right with time. The top edge of the exposed portion is the entrance end of the drift tube at the diode. The bottom edge is the far end of the drift tube. Thus, the slope that the left-most edge of light makes with the vertical is a measure of the transit velocity of the front of the beam. The gross velocity as a function of position down the drift tube, at least for the last four-fifths of the tube, is remarkably constant for all pictures taken at pressures above 0.2 torr. The very fine lines in the streak represent the three joints between the sections of lucite drift tube and they serve as distance markers.

A prominent feature in these streak photographs is the periodicity of the light output as a function of position along the tube. These striation-like features are nearly stationary in the laboratory frame but do shift position during the transit of the beam. This structure can be observed also in the time-integrated pictures, as shown in the second photograph of Figure 4, but here the light is that

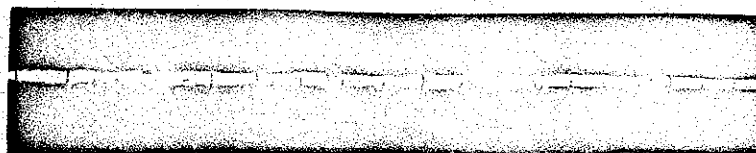
75 nsec.  
 Time



a) Streak photograph of the 6.4 m drift tube with 100 nsec/cm sweep.



b) Open-shutter photograph of the third quarter of the drift tube.



c) Open-shutter photograph of the entire drift tube.

Fig. 4 Records of the visible light from a drift tube filled with 350 m torr of air and guiding a 450 KeV, 48 KA beam.

from the long afterglow following the beam where the light output reflects the final state of the background plasma after the transit of the beam. Care should be taken not to immediately associate this observation with pinching of the beam because any uniform decrease in the light from one position to the next would give the impression of a reduced beam diameter. The distance between adjacent dark spaces along the drift tube is inversely proportional to the pressure, as can be seen in Figure 5. These dark space repetition distances are actually an average of the repetition lengths over the last two-thirds of the drift tube because the separation varies somewhat along the drift tube, becoming shorter near the end. There is also some indication that these lengths are a function of current, decreasing with increasing current.

#### Magnetic Field Probes

Small loop probes distributed along the length of the drift tube were used to measure the magnetic field just inside the conducting screen drift-tube lining. From measurements of the magnetic field, the total current flowing within the drift tube can be determined. These small probes generate a signal proportional to the time derivative of the magnetic field, since  $L/R$  for the probe is less than the shortest time scale in the experiment. This signal is integrated with an RC network, [19] with time constants of a few microseconds and rise times of the order of 3 nsec. The calibration of this probe is dependent on the effective area of the loop and the RC time constant of the integrator. Each of the magnetic field probes were calibrated by placing them in a coaxial line, whose outer diameter was equivalent to the drift tube, and pulsing the line with a known current. Further confirmation that these probes, when observing a beam, were actually measuring magnetic field was obtained from the fact that rotating the loop from a plane through the

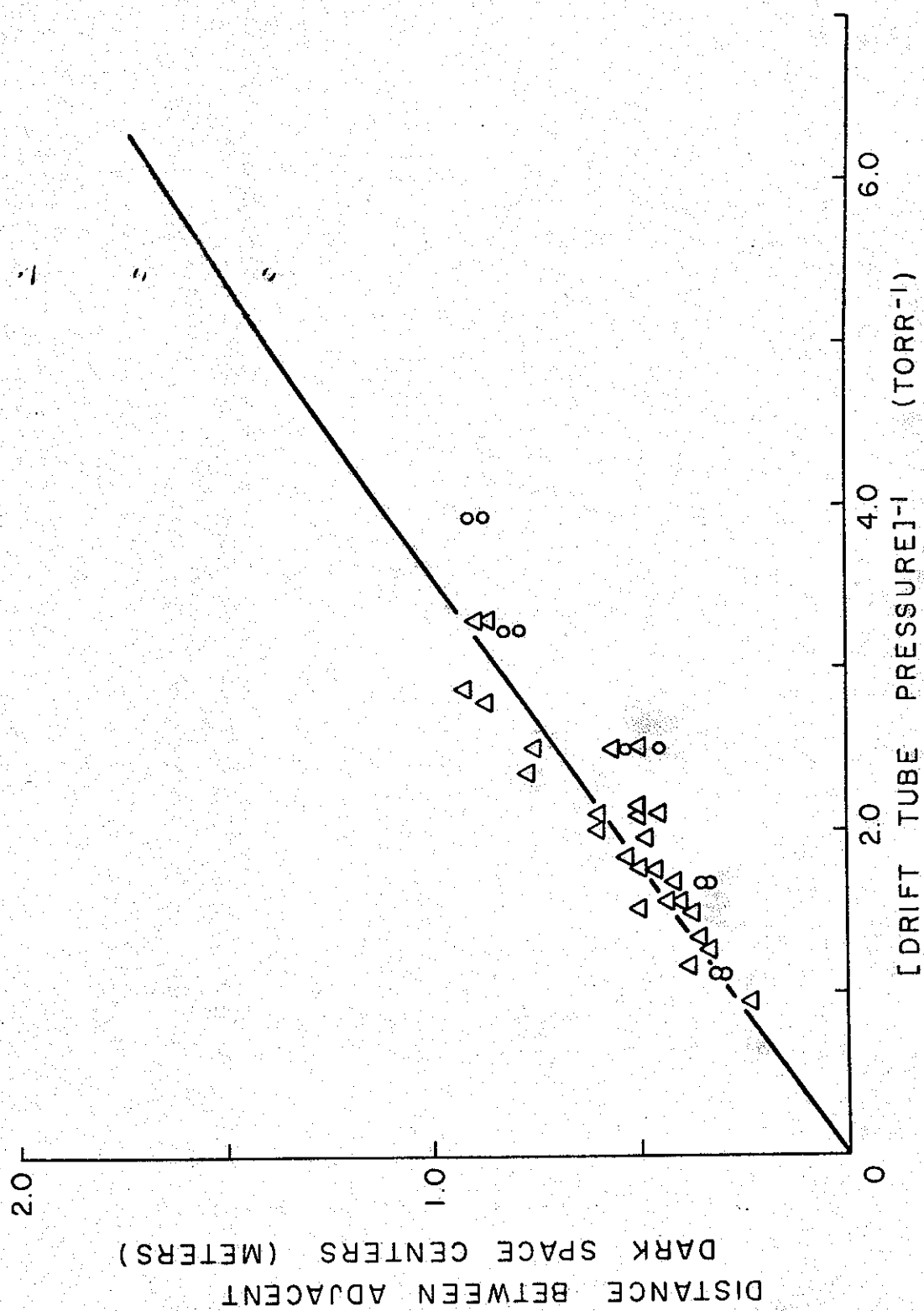
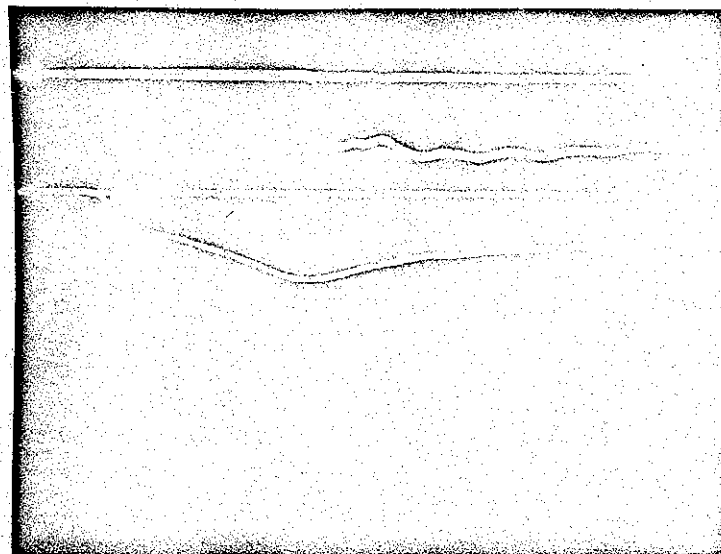
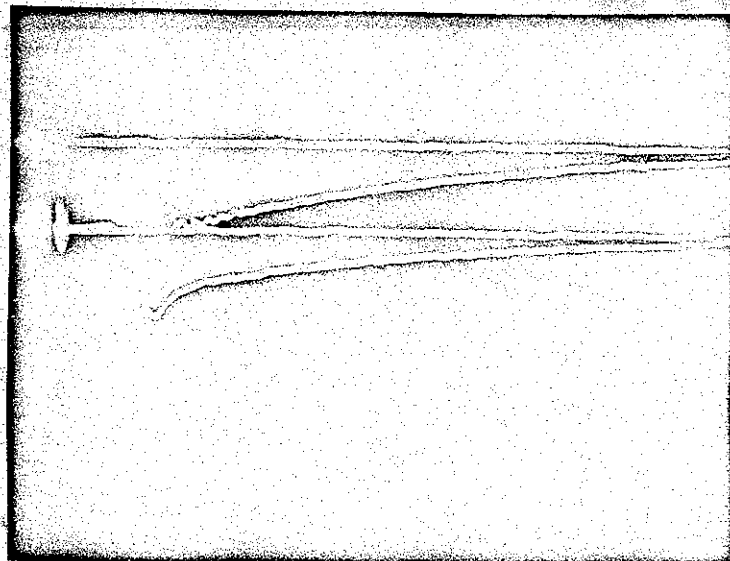


Figure 5 Striatron like noding distance as an inverse function of pressure. The points marked Δ correspond to data where the average energy and current were 450 keV and 35 kA while those marked ○ were 350 keV and 40 kA.





(a) Magnetic field probe traces with a sweep speed of 20 nsec/div. The upper trace is 5.9 m and the lower trace is 0.7 m down the drift tube.



(b) The same traces as (a) except on 100 nsec/div. The fine ripples come from the tees between scopes.

Figure 6 Scope signals from the magnetic field probes. In this case there was 0.88 torr of air in the drift tube and the initial electron energy was 340 keV with a 50 kA peak current.

drift tube axis to a plane perpendicular to the drift tube axis resulted in signals less than 5% of the original. The signals obtained with these loops agreed precisely with the shape of the wall current signal observed from resistive shunts inserted in a break in the wall. When placed outside the conducting wall, the loop probes did not detect any magnetic field. In order that the magnetic fields measured can be related to the current inside the drift tube, two diametrically opposite loop probes were added through a power divider to cancel, in first order, the effects of non-axially symmetric currents. This measured current is not the beam current along the drift tube axis alone, but is the net current within the drift tube, which is a sum of the beam current and any plasma currents present. Since the net current within the drift tube is equal and opposite to the wall current traveling in the screen liner, the two terms are often used interchangeably. Because there tend to be current asymmetries, even at the diode, measurements on opposite sides of the drift tube can give differences of  $\pm 20\%$  from the average. Thus, the error limits assigned to the current measurements must be of this order.

A typical set of signals is displayed in Figure 6 for two of the doublet loop probes. The lower trace in each photograph refers to a probe 0.7 m from the diode, while the upper trace results from a probe 5.9 m down the drift tube near its end. The currents measured by these probes, as seen on the upper photograph with a 20 nsec/div time scale, show rise times approximately independent of pressure above 0.5 torr. At lower pressures these rise times become considerably longer. In addition, the rise times are dependent on position along the drift tube, rising faster nearer the end of the drift tube. The decay times for the currents seen in the lower photograph on 100 nsec/div are much longer than the life of the primary beam. Decay times are independent of the position down the tube but vary strongly with pressure from about 200 nsec at 2.5 Torr to 700 nsec at 0.3 torr. The transit

time of the net current flowing inside the drift tube can also be measured from delay times between the half-rise on the time-synchronized top photograph.

#### Coordinated Results:

These transit times are plotted as a function of pressure in Figure 7 along with measurements of transit time by x-rays from wall foils and light on streak photographs. The agreement between these three methods is quite good, showing a definite increase in transit time with decreasing pressure. Surprisingly long transit times are measured at low pressures. Another measurement derived from these probes is the determination of the wall current as depicted in Figure 8 and 9. In Figure 8 the wall current for different positions along the drift tube is measured as a function of pressure, showing a maximum in the wall current occurring at low pressure. The critical current  $I_c$  with 350 kV on the diode is 23 kA. For Figure 9 the wall current data has been plotted as a function of position, revealing a very sharp drop in wall current within the first meter of the drift tube.

A peculiar phenomena was observed at low pressure which may well be the low-pressure continuation of the periodic bright regions recorded in the photographs of Figure 4. In Figure 10a a streak photograph of the drift tube taken at about 0.1 torr shows a sudden step in the light output of the beam. A closer look at this event, with three magnetic probes, is shown in the four pictures of Figure 10b. These magnetic probes are all time synchronized, each on its own scope, with the same scintillator diode detecting x-rays from a wall foil so that the probes can be cross-correlated in time. The center magnetic probe sits approximately at the step shown in the streak photograph, while the first probe is 0.6 m in front of the step and the third probe is 0.9 m downstream from the step. A striking difference is observed in the rise times of the wall-current signals for the three

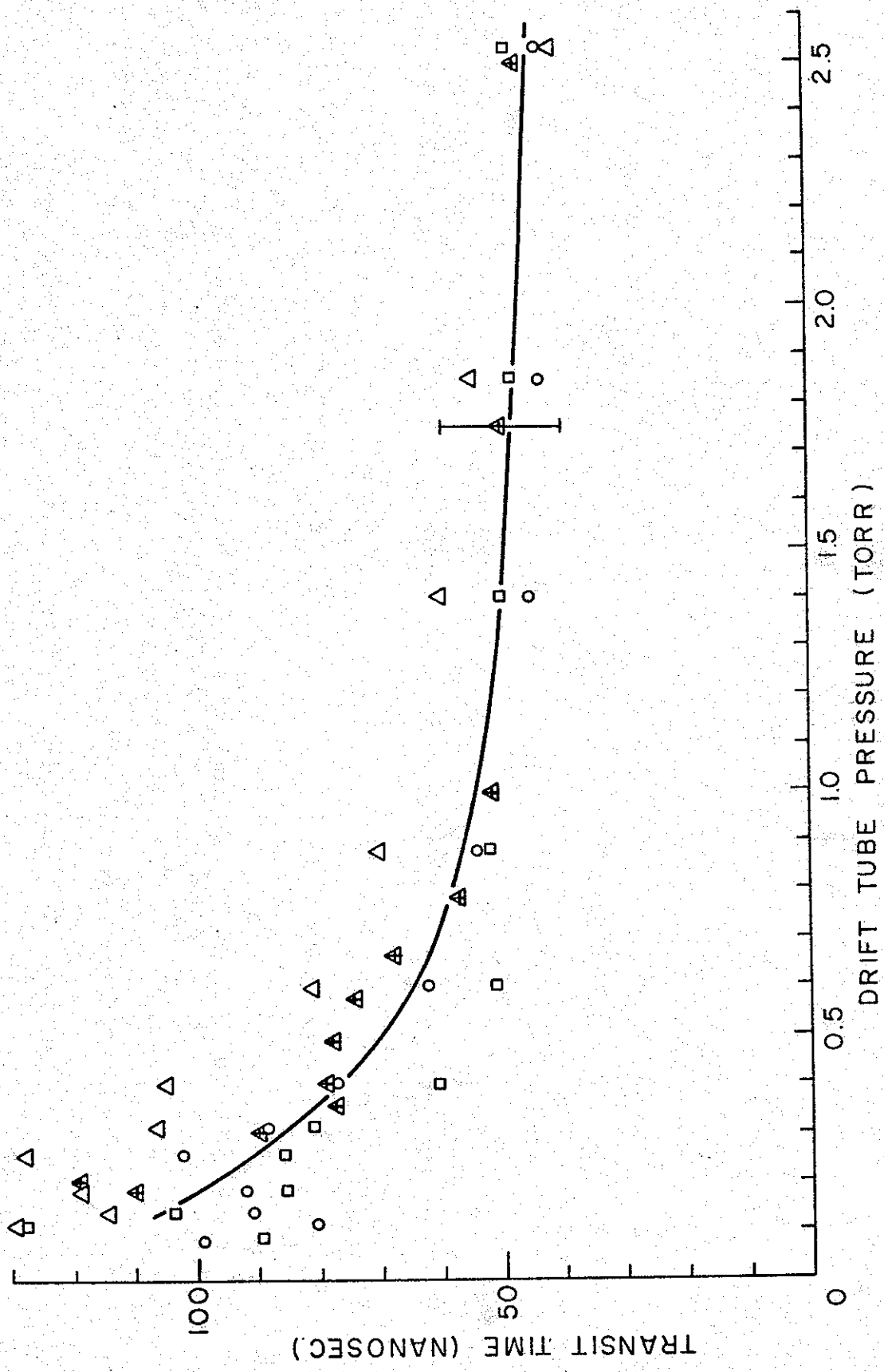


Figure 7 Beam-front transit time as a function of pressure for  $\square$  wall foils,  $\circ$  magnetic field probes, and  $\Delta$  streak photography in a series where the average energy and current were 350 keV and 40 kA. The streak photography data  $\Delta$ , is from a series with 450 keV and 30 kA beams.

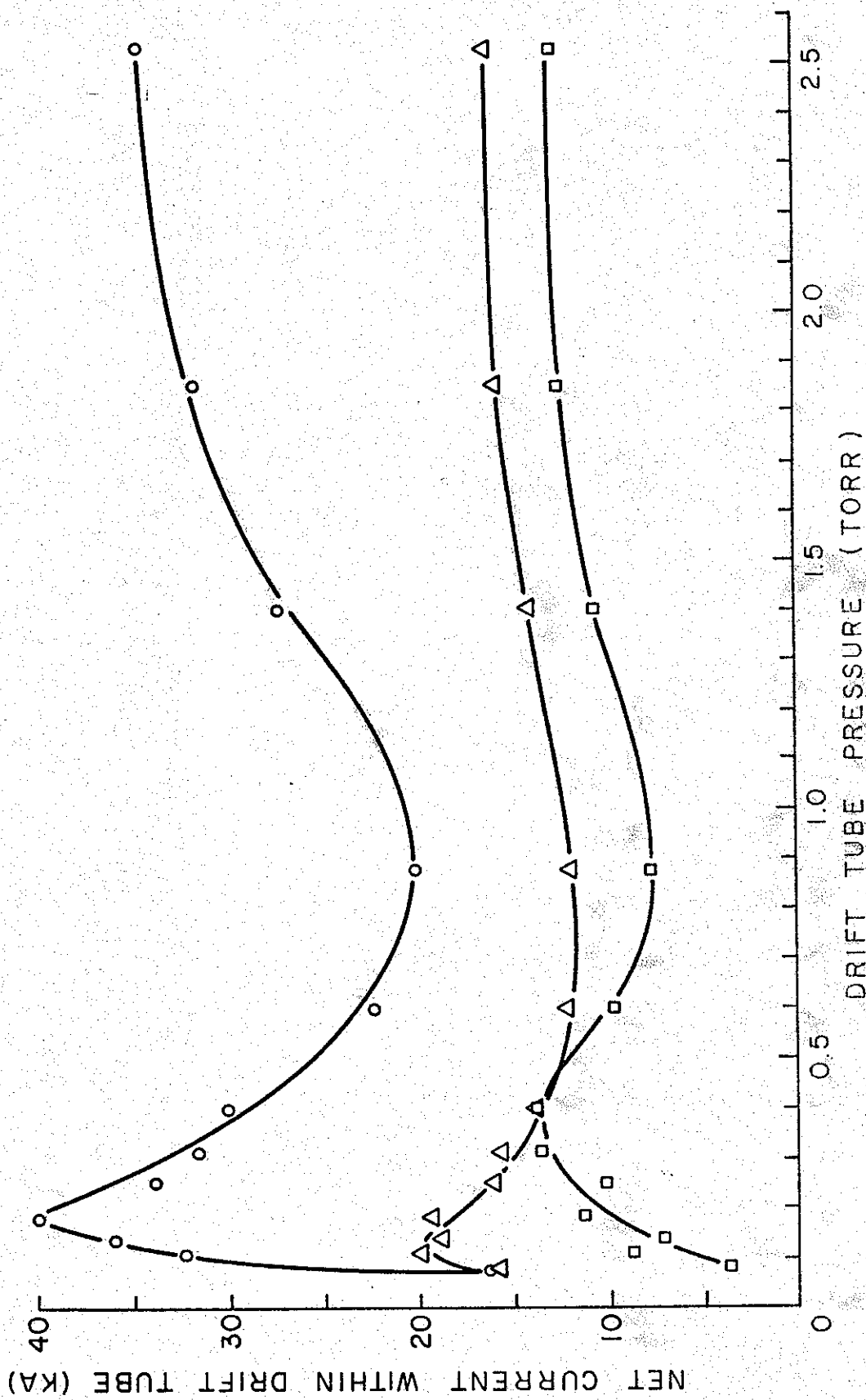


Figure 8 The net current within the drift tube or equivalently the wall current in the screen, as a function of air pressure, at three positions along the drift tube: O - 0.1 m, Δ - 0.7 m, and □ - 4.1 m.

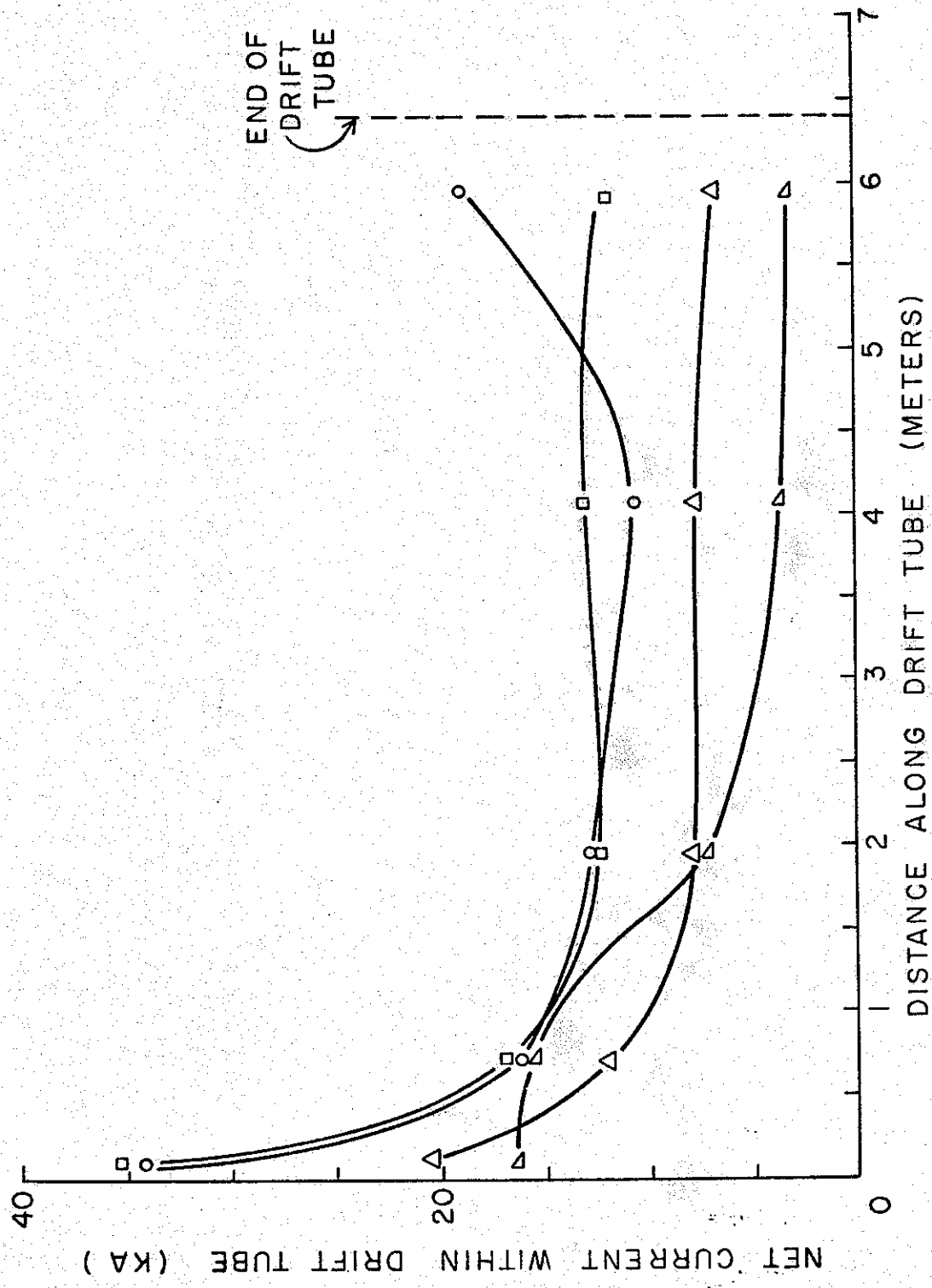
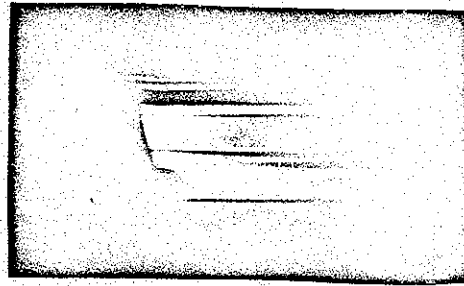
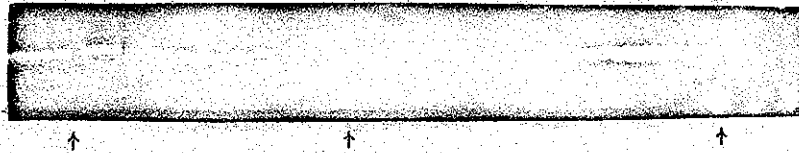


Figure 9 The net current within the drift tube versus position along the drift tube for air pressures of:  $\Delta$  - 88 m Torr,  $\circ$  - 255 m Torr,  $\Delta$  - 880 m Torr and  $\square$  - 2.53 Torr.



(a) Streak and open shutter photographs of a 310 keV 47 kA beam in 135 torr of air. The streak rate is 100 nsec/cm.



(b) Close up observation of the step with three magnetic field probes time synchronized by a single wall foil scintillator diode. Probe positions are indicated by the arrows corresponding to the scope trace directly below. The sweep speed is 50 nsec/div.

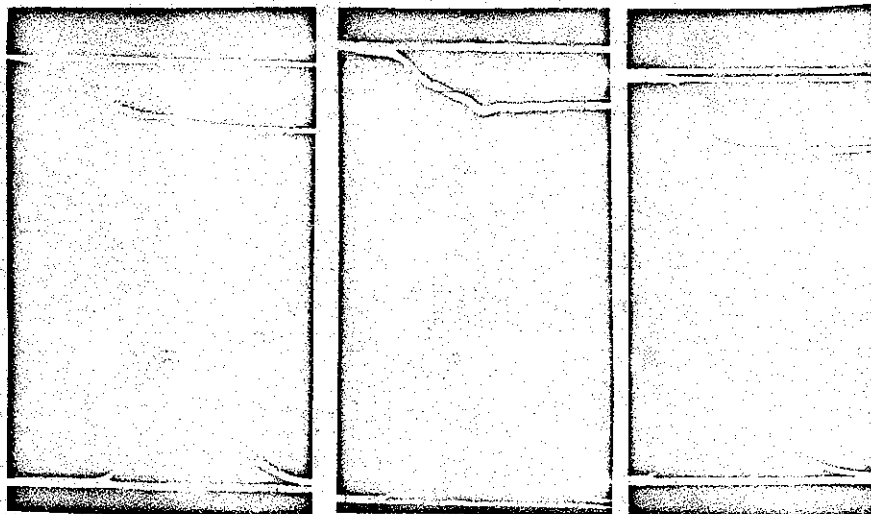


Figure 10 The electron beams at lower pressure show a step discontinuity in propagation.

positions relative to this step. The initial edge of the wall-current signal undergoes more than a 50 nsec delay between probes one and three, a distance of only 1.5 m.

### Discussion

The transit times of a beam through the drift tube, as measured by three diagnostic methods, are always greater than the straight-line trajectory time for 350 kV electrons. At low pressures the transit times exceed the straight line trajectory time by factors of about four. Since these results are preliminary, the explanations are tentative and there are at least three different approaches which may explain the long transit times. The slow propagation time of the beam may be explicable in terms of a loss of electrons to the walls from the front of the beam. Thus, although the beam electrons travel with a high velocity, the effective beam front travels more slowly as the forward-most electrons are continually lost, due to unneutralized electrostatic repulsion at the beam head. A difficulty develops with this interpretation, since at low pressures the transit times are longer than the straight-trajectory time plus the beam duration. This could be explained if one postulated a mechanism for decelerating the primary electrons in the very first part of the drift tube allowing constant velocity thereafter. Such reasoning would also require a special process at the end of the drift tube for reaccelerating the electrons to agree with the speculative results of Table I.

Another theory for the transit times suggests that the electrons have an appreciable amount of transverse energy and their trajectories result in an average velocity along the drift tube considerably smaller than the electron speed along the trajectory. The Alfven-Lawson beam model has a self-consistent solution only for small transverse energies, however, the Hammer-Rostoker [13] model involving hollow beams is applicable and can provide slower propagation times. A problem



also occurs in this explanation though, when one attempts to develop a pressure dependence that fits Figure 7 without including the return secondary current. A third possibility for long transit times involves the experimental observation of a step-like motion of the beam. Such a motion could account for the repetitive bright and dark sections of the drift tube shown in the streak photographs. To make this process feasible, a non-linear mechanism is required which, for example, could cause a rapid increase in the production of the background plasma that suddenly quenches itself and then repeats the sequence. One such mechanism involves coherent Cherenkov radiation from the beam plasma system of such intensity that it would serve to ionize the background gas. [20, 21]

Any explanation for the observed transit times must also be compatible with other behavior such as a constant half-width of the end x-ray pulse which is independent of pressure, and microwave radiation emanating from the drift tube concurrent with the arrival of primary electrons. [22] It may indeed be the case that the propagation of the beam is a combination of the three processes mentioned earlier, such that, at low pressures where neutralization is least rapid, the loss of the front end of the beam to the walls contributes strongly to the long transit times. At slightly higher pressures, particularly near the beginning of the drift tube where the wall current is large, the Hammer-Rostoker beam configuration may exist whose propagation is characterized by highly transverse electron trajectories. For long drift-tube lengths, the step-like configuration of the beam may be most important in determining the travel time.

REFERENCES

1. W. H. Bennett, Phys. Rev. 45, 890 (1934); Phys. Rev. 98, 1584 (1955); Proc. of the 2nd Intl. Conf. U.N. Peaceful Uses of Atomic Energy, Geneva, 32, 451 (1958).
2. H. Alfven, Phys. Rev. 55, 425 (1939).
3. J. D. Lawson, J. Elect. and Control, 3, 587 (1957); J. Elect and Control, 5, 146 (1958); J. Nuc. Energy, Part C, 1, 31 (1959).
4. S. Graybill, J. Uglam and S. Nablo, Bull. A.P.S., 13, 56 (1968).
5. S. Linke, Laboratory of Plasma Studies Annual Report, (1968).
6. S. E. Graybill and S. V. Nablo, Appl. Phy. Letters, 8, 18 (1966).
7. W. T. Link, IEEE Transactions on Nuclear Science, June 1967, p. 777.
8. F. M. Charbonnier, J. P. Barhous, J. L. Brewster, W. P. Dyke and F. J. Grundhauser, IEEE Transactions on Nuclear Science, June 1967, p. 789.
9. T. G. Roberts and W. H. Bennett, Plasma Physics, 10, 381 (1968).
10. T. Martin, D. Johnson and K. Prestwich, Sandia Corporation, Private Communication.
11. J. C. Martin and Co-workers, A. W. R. E., Aldermaston, England, Private Communications.
12. L. P. Bradley and J. C. Ingraham, Conference on Intense Relativistic Electron Beams, Cornell University, January 1969, (unpublished).
13. D. Hammer and N. Rostoker, Bull. A. P. S., Paper 7E4, 13, 1571 (1968).
14. M. L. Andrews, J. J. Bzura, H. E. Davitian, H. H. Fleischmann and D. A. Hammer, Bull. A. P. S., Paper 7E6, 13, 1572 (1968).
15. L. S. Levine, I. M. Vitkovitsky, M. L. Andrews and D. A. Hammer, Bull. A. P. S. Paper 7E7, 13, 1572 (1968).
16. J. J. Clark, D. A. Hammer, S. Linke and M. Ury, Bull. A. P. S., Paper 7E5, 13, 1571 (1968).
17. J. J. Clark, M. Ury, M. L. Andrews, D. A. Hammer and S. Linke, Proc. of the 10th Symposium on Electron, Ion and Laser Beam Technology, N. B. S., Gaithersbury, Maryland, May 1969.
18. H. E. Davitian, Masters Thesis, Department of Applied Physics, Cornell University, January 1969.

19. These integrators were designed by J. Shipman and loaned to us from the Naval Research Laboratory.
20. B. J. Eastlund, Bull. A. P. S., 13, 1532 (1968).
21. B. J. Eastlund and J. M. Wachtel, to be published.
22. J. A. Nation, Bull. A. P. S., Paper 7E8, 13, 1572 (1968).

Unclassified

Security Classification

DOCUMENT CONTROL DATA - R & D

(Security classification of title, body of abstract and indexing annotation must be entered when the overall report is classified)

|                                                                                                                            |                                                           |
|----------------------------------------------------------------------------------------------------------------------------|-----------------------------------------------------------|
| 1. ORIGINATING ACTIVITY (Corporate author)<br>Laboratory of Plasma Studies<br>Cornell University<br>Ithaca, New York 14850 | 2a. REPORT SECURITY CLASSIFICATION<br><b>Unclassified</b> |
|                                                                                                                            | 2b. GROUP                                                 |

3. REPORT TITLE  
**AN INITIAL STUDY ON THE PROPAGATION OF A HIGH CURRENT RELATIVISTIC ELECTRON BEAM**

4. DESCRIPTIVE NOTES (Type of report and, inclusive dates)

5. AUTHOR(S) (First name, middle initial, last name)  
 Merrill L. Andrews      Hans H. Fleischmann      Igor M. Vitkovitsky  
 John J. Bzura          David A. Hammer          Leslie S. Levine  
 Harry E. Davitian

|                                         |                                     |                              |
|-----------------------------------------|-------------------------------------|------------------------------|
| 6. REPORT DATE<br><b>September 1969</b> | 7a. TOTAL NO. OF PAGES<br><b>25</b> | 7b. NO. OF REFS<br><b>22</b> |
|-----------------------------------------|-------------------------------------|------------------------------|

|                                                                                         |                                                                             |
|-----------------------------------------------------------------------------------------|-----------------------------------------------------------------------------|
| 8a. CONTRACT OR GRANT NO.<br><b>N00014-67-A-0077-0003</b><br>b. PROJECT NO.<br>c.<br>d. | 9a. ORIGINATOR'S REPORT NUMBER(S)<br><b>LPS 15</b>                          |
|                                                                                         | 9b. OTHER REPORT NO(S) (Any other numbers that may be assigned this report) |

10. DISTRIBUTION STATEMENT  
 Qualified requestors may obtain copies of this report by writing to  
 Director, Laboratory of Plasma Studies, Upson Hall, Cornell University, Ithaca, N. Y.  
 14850

|                                        |                                                                                                                              |
|----------------------------------------|------------------------------------------------------------------------------------------------------------------------------|
| 11. SUPPLEMENTARY NOTES<br><b>None</b> | 12. SPONSORING MILITARY ACTIVITY<br><b>Plasma Physics Division<br/>Naval Research Laboratory<br/>Washington, D. C. 20390</b> |
|----------------------------------------|------------------------------------------------------------------------------------------------------------------------------|

13. ABSTRACT  
 The transport of relativistic electron beams consisting of up to 500 keV electrons in tens of kiloampere currents has been examined in an introductory experiment with background air pressures of 0.1 to 2.0 torr. These beams were guided in 14cm-diameter metal-mesh-lined lucite drift tubes, typically 6.4 meters long. Their properties were determined through (a) time-resolved measurements of diode voltage and current, (b) x-rays from primary electrons hitting targets along the drift tube walls and at its end, (c) prompt visible light radiated from the beam system recorded in streak photography, and (d) magnetic fields of the total current within the drift tube. Beam-transit times given by these measurements proved to be considerably longer than the straight-line transit of 300 keV electrons, especially at lower pressures. The total current within the drift tube was found to be less than the injected primary electron current, indicating that a large return current was flowing in the beam-produced background plasma that partly canceled the beam current. In the streak photography a striation-like structure was recorded in the light output from the beam and the node-node distance separating these striations varied inversely as the pressure. The implications of these results on possible models for beam propagation are discussed.

| 14. KEY WORDS                                                                                                 | LINK A |    | LINK B |    | LINK C |    |
|---------------------------------------------------------------------------------------------------------------|--------|----|--------|----|--------|----|
|                                                                                                               | ROLE   | WT | ROLE   | WT | ROLE   | WT |
| Plasma Physics<br>Relativistic Electron Beam Propagation<br>Beam Transit Times<br>Beam Current Neutralization |        |    |        |    |        |    |